

PHENOMENOLOGICAL STUDIES OF TOP PAIR  
PRODUCTION AT NEXT-TO-LEADING ORDER\* \*\*

MALGORZATA WOREK

Fachbereich C Physik, Bergische Universität Wuppertal  
42097 Wuppertal, Germany  
worek@physik.uni-wuppertal.de*(Received October 25, 2011)*

The calculation of NLO QCD corrections to the  $t\bar{t} \rightarrow W^+W^-b\bar{b} \rightarrow e^+\nu_e\mu^-\bar{\nu}_\mu b\bar{b}$  process with complete off-shell effects, is briefly summarized. Besides the total cross-section and its scale dependence, a few differential distributions at the Tevatron Run II and LHC are given. All results presented in this contribution have been obtained with the help of the HELAC-NLO Monte Carlo framework.

DOI:10.5506/APhysPolB.42.2415

PACS numbers: 12.38.Bx, 14.65.Ha, 14.80.Bn

**1. Introduction**

The Large Hadron Collider (LHC), with its two main multipurpose detectors ATLAS and CMS, is the experimental project that dominates present particle physics and will likely dominate its next 20–25 years. With the successful start of collisions at 7 TeV, the LHC has put yet another big step towards a thorough examination of the Terascale. Ultimately, it has replaced the older, lower-energy Tevatron, which has been closed in September this year. The large energy available at the LHC has opened many multi-particle channels that are now to a large degree scrutinized. The immense amount of available phase space, and the large acceptance of the ATLAS and CMS detectors allow for the production and identification of final states with 4 or more QCD jets together with isolated leptons. These multi-particle events hide or strongly modify all possible signals of physics beyond the Standard Model. In view of a correct interpretation of the signals of new physics which might be extracted from data, it is of considerable interest to reduce

---

\* Presented at the XXXV International Conference of Theoretical Physics “Matter to the Deepest”, Ustroń, Poland, September 12–18, 2011.

\*\* Preprint number: WUB/11-17.

our theoretical uncertainty for the physical processes under study, especially when large QCD backgrounds are involved. In this respect, the need of next-to-leading-order (NLO) corrections for the LHC is unquestionable.

Efficient numerical evaluation of multi-particle final states at NLO QCD can be performed with the help of the HELAC-NLO Monte Carlo program [1]. HELAC-NLO is an extension of the HELAC-PHEGAS Monte Carlo program [2,3,4], which is based on off-shell Dyson–Schwinger recursive equations. It can be used to efficiently obtain helicity amplitudes and total cross-sections for arbitrary multiparticle processes in the Standard Model and has been already extensively used and tested, see *e.g.* [5,6,7,8,9,10]. Virtual corrections are obtained using the HELAC-1LOOP program [11], based on the

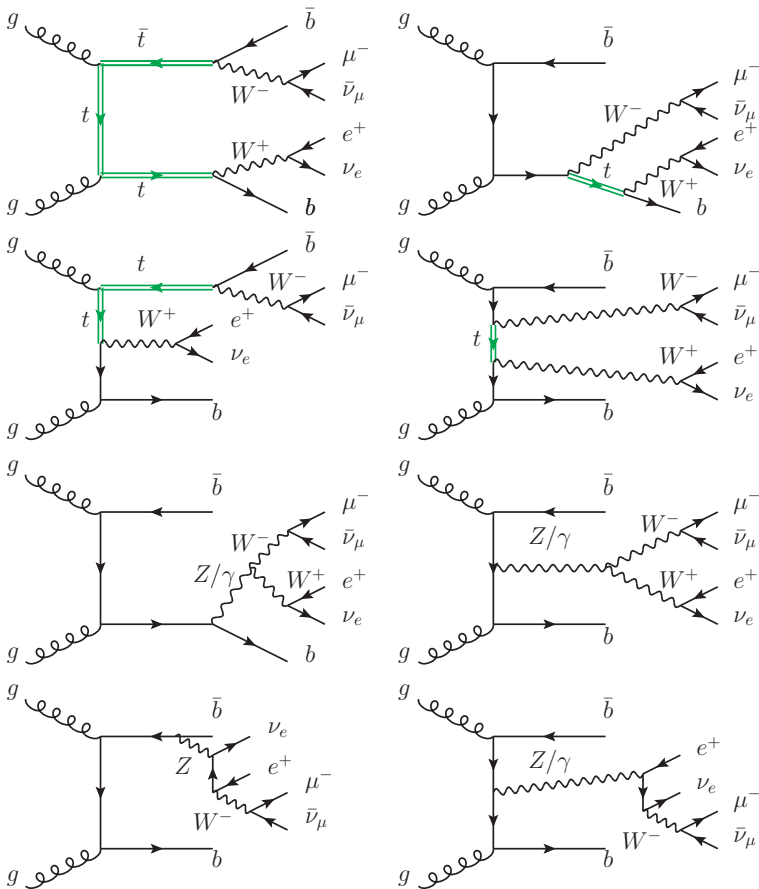


Fig. 1. Representative Feynman diagrams contributing to the leading order process  $gg \rightarrow e^+ \nu_e \mu^- \bar{\nu}_\mu b \bar{b}$  at  $\mathcal{O}(\alpha_s^2 \alpha^4)$ , with different off-shell intermediate states: double-, single-, and non-resonant top quark contributions.

Ossola–Papadopoulos–Pittau (OPP) reduction technique [12] and the reduction code CUTTOOLS [13,14,15,16,17]. Moreover, the ONELoop library [18] has been used for the evaluation of the scalar integrals. Reweighting techniques, helicity and colour sampling methods are used in order to optimize the performance of the system. In addition, the singularities from soft or collinear parton emission are isolated via Catani–Seymour dipole subtraction for NLO QCD calculations using a formulation for massive quarks [19,20] and for arbitrary polarizations [21]. Calculations of this part are performed with the help of the HELAC-DIPOLES software [21]. The optimization and phase space integration is executed with the help of PARNI [22] and KALEU [23]. All parts of the HELAC-NLO framework are publicly available<sup>1</sup>.

With the help of the HELAC-NLO system several  $2 \rightarrow 4$  processes have recently been calculated at next-to-leading order QCD, including  $t\bar{t}b\bar{b}$  [24],  $t\bar{t}jj$  [25,26] and  $W^+W^-b\bar{b}$  [27]. In this contribution, a brief report on the  $pp(p\bar{p}) \rightarrow t\bar{t} \rightarrow W^+W^-b\bar{b} \rightarrow e^+\nu_e\mu^-\bar{\nu}_\mu b\bar{b}$  computation with complete off-shell effects is given. Double-, single- and non-resonant top contributions of the order  $\mathcal{O}(\alpha_s^3\alpha^4)$  are consistently taken into account, which requires the introduction of a complex-mass scheme for unstable top quarks. Moreover, the intermediate  $W$  bosons are treated off-shell. A few examples of Feynman diagrams contributing to the leading order  $gg \rightarrow e^+\nu_e\mu^-\bar{\nu}_\mu b\bar{b}$  subprocess are presented in Fig. 1.

Parallel to our work, another NLO study of  $t\bar{t}b\bar{b}$  [28,29,30] at the LHC appeared. Moreover, NLO QCD corrections to the  $W^+W^-b\bar{b}$  [31] process have been calculated.

## 2. Numerical results

The process  $pp(p\bar{p}) \rightarrow t\bar{t} + X \rightarrow W^+W^-b\bar{b} + X \rightarrow e^+\nu_e\mu^-\bar{\nu}_\mu b\bar{b} + X$  is considered, both at the Tevatron Run II and the LHC *i.e.* at a center-of-mass energy of  $\sqrt{s} = 1.96$  TeV and  $\sqrt{s} = 7$  TeV, correspondingly. The Standard Model parameters are as follows

$$m_W = 80.398 \text{ GeV}, \quad \Gamma_W = 2.141 \text{ GeV}, \quad (2.1)$$

$$m_Z = 91.1876 \text{ GeV}, \quad \Gamma_Z = 2.4952 \text{ GeV}, \quad (2.2)$$

$$G_\mu = 1.16639 \times 10^{-5} \text{ GeV}^{-2}. \quad (2.3)$$

The electromagnetic coupling and  $\sin^2\theta_W$  are derived from the Fermi constant and masses of  $W$  and  $Z$  bosons. The top quark mass is  $m_t = 172.6$  GeV and all other QCD partons and leptons are treated as massless. The top quark width is  $\Gamma_t^{\text{LO}} = 1.48$  GeV at LO and  $\Gamma_t^{\text{NLO}} = 1.35$  GeV at NLO, where  $\alpha_s = \alpha_s(m_t) = 0.107639510785815$ . The on-shell scheme is adopted

<sup>1</sup> <http://helac-phegas.web.cern.ch/helac-phegas/>

for mass renormalization. All final-state partons with pseudorapidity  $|\eta| < 5$  are recombined into jets via the  $k_T$  algorithm [32, 33, 34], the *anti- $k_T$*  algorithm [35] and the inclusive Cambridge/Aachen algorithm (C/A) [36] with a cone of size  $R = 0.4$ . Additional cuts are imposed on the transverse momenta and the rapidity of two recombined  $b$ -jets

$$p_{T_b} > 20 \text{ GeV}, \quad |y_b| < 4.5. \quad (2.4)$$

Basic selection is applied to decay products of top quarks

$$p_{T_\ell} > 20 \text{ GeV}, \quad |\eta_\ell| < 2.5, \quad \Delta R_{b\ell} > 0.4, \quad p_{T_{\text{miss}}} > 30 \text{ GeV}. \quad (2.5)$$

The CTEQ6 set of parton distribution functions (PDFs) is consistently used [37, 38]. In particular, CTEQ6L1 PDFs with a 1-loop running  $\alpha_s$  is taken at LO and CTEQ6M PDFs with a 2-loop running  $\alpha_s$  at NLO. The contribution from  $b$  quarks in the initial state is neglected. The number of active flavors is  $N_F = 5$ , and the respective QCD parameters are  $\Lambda_5^{LO} = 165$  MeV and  $\Lambda_5^{\text{MS}} = 226$  MeV. In the renormalization of the strong coupling constant, the top-quark loop in the gluon self-energy is subtracted at zero momentum. In this scheme the running of  $\alpha_s$  is generated by the contributions of the light-quark and gluon loops. The renormalization and factorization scales,  $\mu_R$  and  $\mu_F$ , are set to the common value  $\mu = m_t$ .

### 2.1. Tevatron Run II

We start with a discussion of the total cross-section at the Tevatron Run II. In spite of the fact that the Tevatron has been recently closed, the data analysis in the CDF and D0 experiments is still ongoing. Therefore, in Table I results for the total cross-section for the central value of the scale,  $\mu_R = \mu_F = m_t$  and for three different jet algorithms:  $k_T$ , *anti- $k_T$*  and the inclusive Cambridge/Aachen algorithm (C/A), are presented. The total cross-section receives small NLO QCD correction of the order of 2%. Residual scale uncertainties, as obtained by varying the scale down and up

TABLE I

Integrated cross-section at LO and NLO for  $p\bar{p} \rightarrow e^+\nu_e\mu^-\bar{\nu}_\mu b\bar{b} + X$  production at the Tevatron Run II.

Algorithm	$\sigma_{\text{LO}}$ [fb]	$\sigma_{\text{NLO}}$ [fb]
<i>anti-<math>k_T</math></i>	$34.922 \pm 0.014$	$35.697 \pm 0.049$
$k_T$	$34.922 \pm 0.014$	$35.723 \pm 0.049$
C/A	$34.922 \pm 0.014$	$35.746 \pm 0.050$

by a factor 2, are at the 40% level in the LO case. The dependence is large, illustrating the well known fact that the LO prediction can only provide a rough estimate. As expected, we observe a reduction of the scale uncertainty while going from LO to NLO. In the NLO case we have obtained a variation of the order of 8%. In addition, the size of the non-factorizable corrections, as obtained by a comparison of the full result against a result in the narrow width approximation (NWA), amounts to 1%. This is consistent with the uncertainty of the NWA *i.e.* which is of the order  $\mathcal{O}(\Gamma_t/m_t)$ .

In the next step, corrections to differential distributions are presented. In Fig. 2, differential cross-section distributions as function of the averaged transverse momentum and averaged rapidity of the charged leptons are

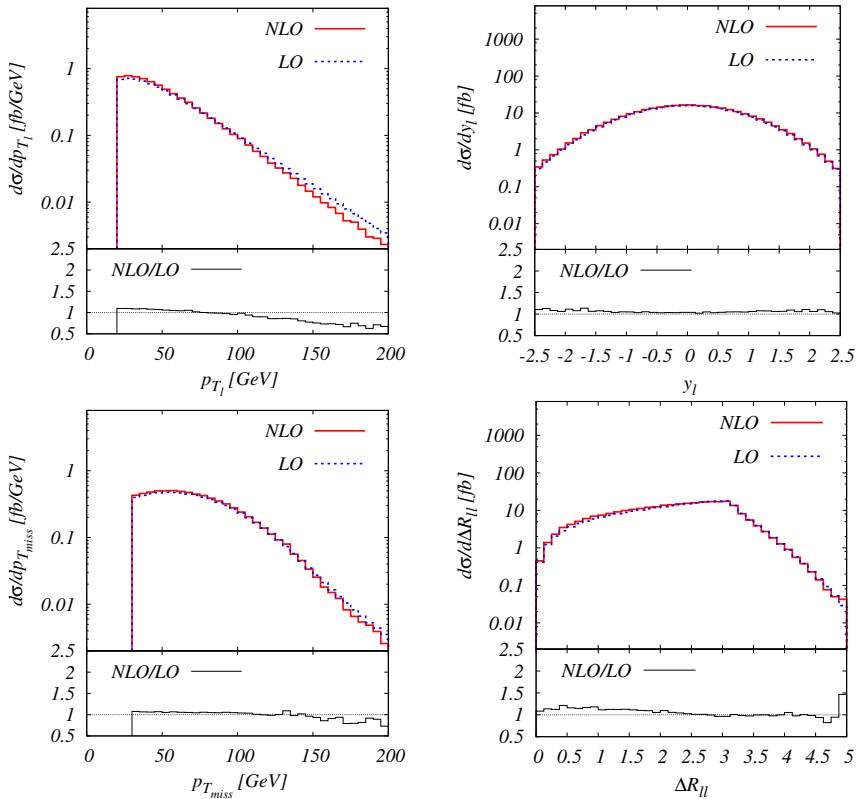


Fig. 2. Differential cross-section distributions as a function of the averaged transverse momentum  $p_{T_\ell}$  of the charged leptons, averaged rapidity  $y_\ell$  of the charged leptons,  $p_{T_{\text{miss}}}$  and  $\Delta R_{\ell\ell}$  for the  $p\bar{p} \rightarrow e^+\nu_e\mu^-\bar{\nu}_\mu b\bar{b} + X$  process at the Tevatron Run II. The dashed (blue) curve corresponds to the leading order, whereas the solid (red) one to the next-to-leading order result. The lower panels display the differential  $K$  factor.

given. Also shown are distributions of missing transverse momentum,  $p_{T_{\text{miss}}}$ , and dilepton separation in the azimuthal angle-pseudorapidity plane,  $\Delta R_{\ell\ell}$ . Even though the NLO corrections to the transverse momentum distribution are moderate, they do not simply rescale the LO shape. A distortion at the level of 40% is induced. For  $p_{T_{\text{miss}}}$ , a distortion only up to 15% can be observed. As for angular distributions positive and rather modest corrections of the order of 5%–10% are obtained.

## 2.2. Large Hadron Collider

Table II shows the integrated cross-sections at the LHC with  $\sqrt{s} = 7$  TeV, for three different jet algorithms. At the central scale value, the full cross-section receives NLO QCD corrections of the order of 47%. After including the NLO corrections, a large scale dependence of about 37% in the LO cross-section is considerably reduced down to 9%.

TABLE II

Integrated cross-section at LO and NLO for  $pp \rightarrow e^+ \nu_e \mu^- \bar{\nu}_\mu b \bar{b} + X$  production at the LHC.

Algorithm	$\sigma_{\text{LO}}$ [fb]	$\sigma_{\text{NLO}}$ [fb]
<i>anti-k<sub>T</sub></i>	$550.54 \pm 0.18$	$808.29 \pm 1.04$
<i>k<sub>T</sub></i>	$550.54 \pm 0.18$	$808.86 \pm 1.03$
C/A	$550.54 \pm 0.18$	$808.28 \pm 1.03$

In order to quantify the size of the non-factorizable corrections for the LHC, a comparison to the narrow-width limit of our calculation has again been performed. Going from NWA to the full result changes the cross-section no more than 1.2% for our inclusive setup.

In Fig. 3, differential cross-section distributions as function of the averaged transverse momentum and averaged rapidity of the charged leptons together with  $p_{T_{\text{miss}}}$  and  $\Delta R_{\ell\ell}$  separation are shown.

For renormalization and factorization scales set to a common value  $\mu = m_t$ , the NLO QCD corrections are always positive and relatively large. In particular, in case of the  $p_{T_\ell}$  differential distribution, a distortion up to 25% is reached, while for  $p_{T_{\text{miss}}}$  a distortion up to 80% is visible. For the  $y_\ell$  distribution, rather constant corrections up to 50% are obtained. And finally, the distribution in  $\Delta R_{\ell\ell}$  has even acquired corrections up to 90%.

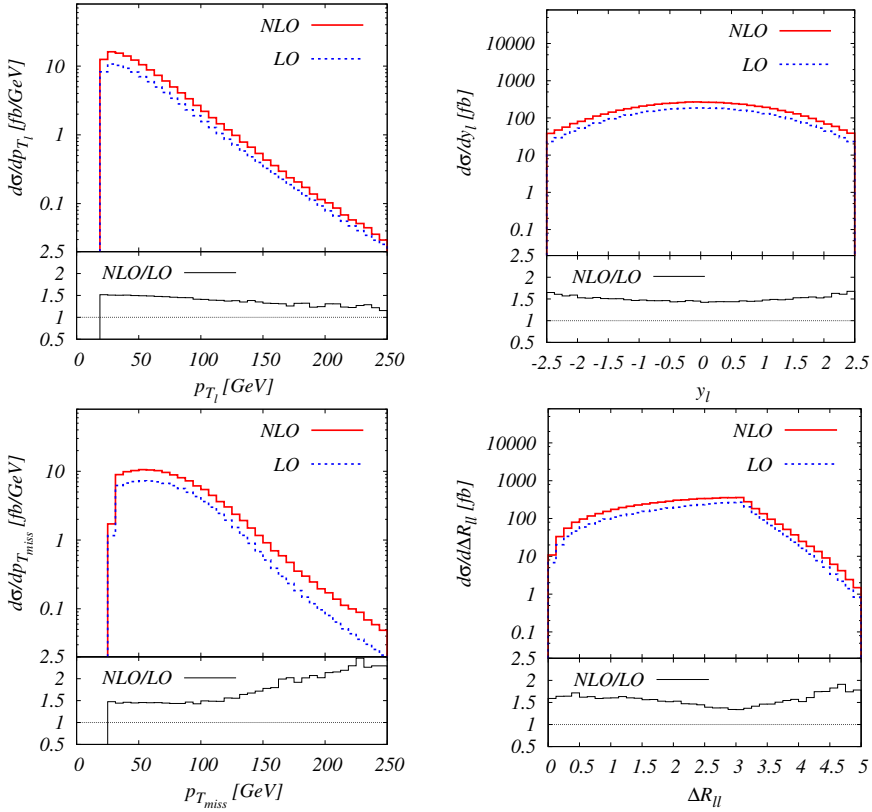


Fig. 3. Differential cross-section distributions as a function of the averaged transverse momentum  $p_{T_\ell}$  of the charged leptons, averaged rapidity  $y_\ell$  of the charged leptons,  $p_{T_{\text{miss}}}$  and  $\Delta R_{\ell\ell}$  for the  $pp \rightarrow e^+ \nu_e \mu^- \bar{\nu}_\mu b\bar{b} + X$  process at the LHC. The dashed (blue) curve corresponds to the leading order, whereas the solid (red) one to the next-to-leading order result. The lower panels display the differential  $K$  factor.

### 3. Summary

The NLO QCD corrections to the full decay chain  $pp(p\bar{p}) \rightarrow t\bar{t} \rightarrow W^+W^-b\bar{b} \rightarrow e^+\nu_e\mu^-\bar{\nu}_\mu b\bar{b} + X$  have been briefly presented. In the calculation, all off-shell effects of top quarks and  $W$  gauge bosons have been included in a fully differential way. The total cross-section and its scale dependence, as well as a few differential distributions at the Tevatron Run II and the LHC have been given. The impact of the NLO QCD corrections on integrated cross-sections at the Tevatron is small, of the order of 2%. On the other hand, at the LHC, 47% NLO QCD corrections have been obtained.

Residual theoretical uncertainties due to higher order corrections have been estimated to be at the 8%–9% level. And finally, NLO QCD corrections do not only affect the overall normalization of the integrated cross-sections, but can also change the shape of some differential distributions.

I would like to thank the Organizers of the XXXV International Conference of Theoretical Physics, Ustroń 2011, for the kind invitation and the very pleasant atmosphere during the conference. The calculations presented here have been performed on the Grid Cluster of the Bergische Universität Wuppertal, financed by the Helmholtz — Alliance “Physics at the Terascale” and the BMBF. The author was supported by the Initiative and Networking Fund of the Helmholtz Association, contract HA-101 (Physics at the Terascale).

## REFERENCES

- [1] G. Bevilacqua *et al.*, arXiv:1110.1499 [hep-ph].
- [2] A. Kanaki, C.G. Papadopoulos, *Comput. Phys. Commun.* **132**, 306 (2000) [arXiv:hep-ph/0002082v2].
- [3] C.G. Papadopoulos, *Comput. Phys. Commun.* **137**, 247 (2001) [arXiv:hep-ph/0007335v1].
- [4] A. Cafarella, C.G. Papadopoulos, M. Worek, *Comput. Phys. Commun.* **180**, 1941 (2009) [arXiv:0710.2427 [hep-ph]].
- [5] T. Gleisberg *et al.*, *Eur. Phys. J.* **C34**, 173 (2004) [arXiv:hep-ph/0311273].
- [6] C.G. Papadopoulos, M. Worek, *Eur. Phys. J.* **C50**, 843 (2007) [arXiv:hep-ph/0512150].
- [7] J. Alwall *et al.*, *Eur. Phys. J.* **C53**, 473 (2008) [arXiv:0706.2569 [hep-ph]].
- [8] C. Englert, B. Jager, M. Worek, D. Zeppenfeld, *Phys. Rev.* **D80**, 035027 (2009) [arXiv:0810.4861 [hep-ph]].
- [9] S. Actis *et al.*, *Eur. Phys. J.* **C66**, 585 (2010) [arXiv:0912.0749 [hep-ph]].
- [10] C.C. Calame *et al.*, *J. High Energy Phys.* **1107**, 126 (2011) [arXiv:1106.3178 [hep-ph]].
- [11] A. van Hameren, C.G. Papadopoulos, R. Pittau, *J. High Energy Phys.* **0909**, 106 (2009) [arXiv:0903.4665 [hep-ph]].
- [12] G. Ossola, C.G. Papadopoulos, R. Pittau, *Nucl. Phys.* **B763**, 147 (2007) [arXiv:hep-ph/0609007].
- [13] G. Ossola, C.G. Papadopoulos, R. Pittau, *J. High Energy Phys.* **0803**, 042 (2008) [arXiv:0711.3596 [hep-ph]].
- [14] P. Draggiotis, M.V. Garzelli, C.G. Papadopoulos, R. Pittau, *J. High Energy Phys.* **0904**, 072 (2009) [arXiv:0903.0356 [hep-ph]].
- [15] M.V. Garzelli, I. Malamos, R. Pittau, *J. High Energy Phys.* **1001**, 040 (2010) [Erratum *ibid.* **1010**, 097 (2010)] [arXiv:0910.3130 [hep-ph]].

- [16] M.V. Garzelli, I. Malamos, R. Pittau, *J. High Energy Phys.* **1101**, 029 (2011) [arXiv:1009.4302 [hep-ph]].
- [17] M.V. Garzelli, I. Malamos, *Eur. Phys. J. C* **71**, 1605 (2011) [arXiv:1010.1248 [hep-ph]].
- [18] A. van Hameren, *Comput. Phys. Commun.* **182**, 2427 (2011) [arXiv:1007.4716 [hep-ph]].
- [19] S. Catani, M.H. Seymour, *Nucl. Phys.* **B485**, 291 (1997) [arXiv:hep-ph/9605323].
- [20] S. Catani, S. Dittmaier, M.H. Seymour, Z. Trocsanyi, *Nucl. Phys.* **B627**, 189 (2002) [arXiv:hep-ph/0201036].
- [21] M. Czakon, C.G. Papadopoulos, M. Worek, *J. High Energy Phys.* **0908**, 085 (2009) [arXiv:0905.0883 [hep-ph]].
- [22] A. van Hameren, *Acta Phys. Pol. B* **40**, 259 (2009) [arXiv:0710.2448 [hep-ph]].
- [23] A. van Hameren, arXiv:1003.4953 [hep-ph].
- [24] G. Bevilacqua *et al.*, *J. High Energy Phys.* **0909**, 109 (2009) [arXiv:0907.4723 [hep-ph]].
- [25] G. Bevilacqua, M. Czakon, C.G. Papadopoulos, M. Worek, *Phys. Rev. Lett.* **104**, 162002 (2010) [arXiv:1002.4009 [hep-ph]].
- [26] G. Bevilacqua, M. Czakon, C.G. Papadopoulos, M. Worek, arXiv:1108.2851 [hep-ph].
- [27] G. Bevilacqua *et al.*, *J. High Energy Phys.* **1102**, 083 (2011) [arXiv:1012.4230 [hep-ph]].
- [28] A. Bredenstein, A. Denner, S. Dittmaier, S. Pozzorini, *J. High Energy Phys.* **0808**, 108 (2008) [arXiv:0807.1248 [hep-ph]].
- [29] A. Bredenstein, A. Denner, S. Dittmaier, S. Pozzorini, *Phys. Rev. Lett.* **103**, 012002 (2009) [arXiv:0905.0110 [hep-ph]].
- [30] A. Bredenstein, A. Denner, S. Dittmaier, S. Pozzorini, *J. High Energy Phys.* **1003**, 021 (2010) [arXiv:1001.4006 [hep-ph]].
- [31] A. Denner, S. Dittmaier, S. Kallweit, S. Pozzorini, *Phys. Rev. Lett.* **106**, 052001 (2011) [arXiv:1012.3975 [hep-ph]].
- [32] S. Catani, Y.L. Dokshitzer, B.R. Webber, *Phys. Lett.* **B285**, 291 (1992).
- [33] S. Catani, Y.L. Dokshitzer, M.H. Seymour, B.R. Webber, *Nucl. Phys.* **B406**, 187 (1993).
- [34] S.D. Ellis, D.E. Soper, *Phys. Rev.* **D48**, 3160 (1993) [arXiv:hep-ph/9305266].
- [35] M. Cacciari, G.P. Salam, G. Soyez, *J. High Energy Phys.* **0804**, 063 (2008) [arXiv:0802.1189 [hep-ph]].
- [36] Y.L. Dokshitzer, G.D. Leder, S. Moretti, B.R. Webber, *J. High Energy Phys.* **9708**, 001 (1997) [arXiv:hep-ph/9707323].
- [37] J. Pumplin *et al.*, *J. High Energy Phys.* **0207**, 012 (2002) [arXiv:hep-ph/0201195].
- [38] D. Stump *et al.*, *J. High Energy Phys.* **0310**, 046 (2003) [arXiv:hep-ph/0303013].